INTERNAL WAVE PROPAGATION

Bruce R. Sutherland

Department of Mathematical and Statistical Sciences
University of Alberta

Abstract

The current development of linear, weakly nonlinear and fully nonlinear theories of the propagation of internal waves in continuously stratified fluid is reviewed and new analyses are presented that demonstrate the usefulness of parcel arguments in developing an intuition for small-amplitude internal wave dynamics. Directions for future research are suggested.

KEYWORDS: internal waves, ray theory, instability

1 Introduction

Internal waves are characterised by periodic undulations within a fluid whose density decreases with height. The governing dynamics are essentially the same as those of surface waves: both move due buoyancy restoring forces. However, whereas surface waves are confined to the interface between water and air, internal waves can propagate both horizontally and vertically.

Internal waves occur throughout the atmosphere and ocean on scales as small as meters and as large as thousands of kilometers. Under suitable atmospheric conditions, clouds help visualise the waves. Where the waves push air upwards near the wave crests the air expands in the lower pressure and it cools due to thermodynamic effects. If the air itself is initially saturated with water vapour, clouds form as the vapour condenses into water droplets in the cooling air. Conversely, the droplets evaporate near the wave troughs where the air moves downwards into higher pressure and so heats up under compression. A typical image of internal waves visualised by clouds is shown in Figure 1.

The equation describing the motion of internal waves in the atmosphere and ocean are given by a remarkably simple set of partial differential equations. The Navier-Stokes equations express conservation of momentum:

$$\rho_{\rm T}\frac{D\mathbf{u}}{Dt} = -\nabla p_{\rm T} + \rho_{\rm T}\mathbf{g} + \mathbf{F}_{\rm rot} + \mu\nabla^2\mathbf{u}. \qquad (1)$$

Fig. 1: Enhanced photograph showing internal waves visualised by clouds as they propagate over floating icepacks in the Arctic ocean. The picture was taken at 9pm GMT July 23, 1999 from an airplane window while flying south of Baffin Island in northern Canada. The wave crests propagate downward and to the right in the picture.

Here $\rho_{\rm T}$ is the density of the fluid, $\mathbf{u} = (u, v, w)$ denote the components of west-to-east (u), south-to-north (v) and vertical (w) motion corresponding to directions $\hat{\mathbf{x}}$, $\hat{\mathbf{y}}$ and $\hat{\mathbf{z}}$, respectively. The pressure is denoted by $p_{\rm T}$, $\mathbf{g} = -g\hat{\mathbf{z}}$ is the acceleration due to gravity, μ is the molecular viscosity, and $\mathbf{F}_{\rm rot}$ denotes external forces that occur due to the Earth's rotation, namely Coriolis forces.

We neglect the effect of vertically propagating sound waves which is done by assuming the fluid is incompressible. Thus the continuity equation, which expresses conservation of mass, is written

$$\frac{D\rho_{\rm T}}{Dt} = 0, \tag{2}$$

and consequently we have

$$\nabla \cdot \mathbf{u} = 0. \tag{3}$$

In these equations the material derivative,

$$\frac{D}{Dt} \equiv \frac{\partial}{\partial_t} + \mathbf{u} \cdot \nabla, \tag{4}$$

introduces nonlinearity through the "advective" terms, denoted by the second term on the right-hand-side of (4).

The five coupled partial differential equations in five unknowns, $(\mathbf{u}, \rho, p)$ describe a wide range of phenomena, including waves and turbulence occurring on length scales as small as millimeters and as large as thousands of kilometers.

In this study, we will focus on internal wave phenomena on scales ranging from tens of meters to planetary scales. A straightforward scaling analysis reveals that viscosity and diffusion (for example of salt water or heat) are negligibly important compared with the advective and pressure gradient terms in the equations.

We further simplify the equations by subdividing the pressure and density fields into background fields ($\overline{p}(z)$ and $\overline{\rho}(z)$, respectively) and perturbation fields ($p(\mathbf{x}, t)$ and $\rho(\mathbf{x}, t)$, respectively), and we assume that the background fields are in "hydrostatic balance". That is, we assume the fields are related by

$$\frac{d\overline{p}}{dz} = -\overline{\rho} g. \tag{5}$$

This is simply the statement that, in a stationary fluid, the pressure at a given vertical level is set by the weight of fluid per unit area lying above that level.

Thus, substituting $\mu = 0$ and $p_{\rm T} = \overline{p} + p$ and $\rho_{\rm T} = \overline{\rho} + \rho$ into (1) gives

$$\rho_{\rm T} \frac{D\mathbf{u}}{Dt} = -\nabla p - \rho g \hat{\mathbf{z}} + \mathbf{F}_{\rm rot}, \tag{6}$$

and the continuity equation becomes

$$\frac{D\rho}{Dt} + w \frac{d\overline{\rho}}{dz} = 0. \tag{7}$$

Further approximations may be employed resulting in different classes of wave motion:

- If one assumes the flow is "hydrostatic" (meaning the perturbation as well as background pressure and density fields are in balance) then one sets $\partial p/\partial z = -\rho g$ in (6). Hydrostatic internal waves propagate with frequencies much smaller than the natural frequency of oscillation of a stratified fluid, the "buoyancy frequency". Waves with frequencies close to the buoyancy frequency are said to be "non-hydrostatic".

- If one assumes the flow is "Boussinesq" (meaning that density variations are important only as they affect the buoyancy term) then one sets $\rho_{\rm T} \to \rho_0$, a constant, in the terms before the material derivatives in (6). Boussinesq internal waves occur in fluids whose density decreases by only a small fraction of the total density with height.

- If one assumes the flow is "anelastic", one instead sets $\rho_{\rm T} \to \overline{\rho}$ in (6). This approximation accounts for the increase in amplitude of waves with altitude in the atmosphere as the density of air decreases by a significant fraction from the troposphere to the middle and upper atmosphere.

- If one assumes the waves are small amplitude, then the nonlinear terms in the material derivative may be neglected. For example, if there is no mean background flow, then $D/Dt \to \partial/\partial t$.

We will consider the consequences of these different approximations in the following sections.

2 Linear Theory

The linear theory for internal waves can be approached either through "fluid parcel" consideration, in which the local forces acting upon an infinitesimal patch of fluid is considered, or through partial differential equations whose solutions express the cumulative effects of conservation principles. Both approaches are discussed below.

2.1 Parcel Arguments

The motion of small amplitude internal waves can be understood in part from a "parcel" argument, as illustrated in Figure 2. Consider first a fluid parcel (a infinitesimal patch of fluid) that is vertically displaced upward by a small amount, δz, in a surrounding stratified fluid whose density, $\overline{\rho}(z)$, decreases linearly with height. The parcel, of density ρ_0, finds itself surrounded by less dense fluid and therefore it experiences a restoring force due to buoyancy. Newton's laws reveal the consequent motion:

$$\rho_0 \frac{d^2\delta z}{dt^2} = -(\delta\rho)g. \tag{8}$$

Here g is the acceleration due to gravity and $\delta\rho$ is the density difference between the fluid parcel and the surrounding fluid at its displaced position. The density difference can be written in terms of δz. Because $|\delta z|$ is infinitessimally small $\delta\rho = -(d\overline{\rho}/dz)\delta z$. Thus (8) becomes

$$\frac{d^2\delta z}{dt^2} + N^2\delta z = 0, \tag{9}$$

in which, by definition

$$N^2 \equiv -\frac{g}{\rho_0}\frac{d\overline{\rho}}{dz}. \tag{10}$$

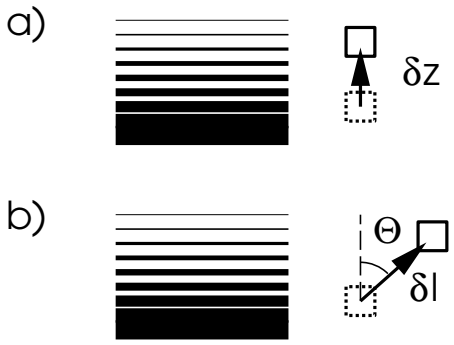

Fig. 2: Schematic illustrating forces acting upon a fluid parcel that is displaced a) vertically and b) at an angle to the vertical in a stratified fluid.

Because (9) is a spring equation, it is apparent that a vertically displaced fluid parcel will oscillate in a linear stratified fluid at a frequency N, which is proportional to the square root of the background density gradient. Consequently, the value N is called the buoyancy frequency (though it is also sometimes called the Brunt-Väisälä frequency after the scientists who first examined these dynamics [75, 9]). Typical values of N in the atmosphere and ocean are around $10^{-2}\,\mathrm{s}^{-1}$, so vertical oscillations occur with a period on the order of tens of minutes.

Now consider the case in which a fluid parcel is displaced a small distance δl along a line at an angle Θ to the vertical, as shown in Fig. 2b. Furthermore, assume that the fluid motion is constrained to move along this line. Although this may seem to be an unphysical assumption, in § 2.3 a fluid parcel displaced by an internal wave is shown to undergo exactly this diagonal linear motion.

Newton's laws for the force along the line give

$$\rho_0 \frac{d^2\delta l}{dt^2} = -(\delta\rho) g \cos\Theta. \tag{11}$$

The $\cos\Theta$ term enters by resolving the downward gravitational force into the along-line direction. As before, $\delta\rho$ can be written in terms of δl by the relation $\delta\rho = -(d\overline{\rho}/dz)\delta l \cos\Theta$. Thus (11) becomes

$$\frac{d^2\delta l}{dt^2} + N^2 \cos^2\Theta \delta l = 0. \tag{12}$$

This new spring equation shows that fluid motion along a line at an angle to the vertical occurs with frequency

$$\omega = N\cos\Theta, \tag{13}$$

which, indeed, is the dispersion relation for internal waves when it is recognised that $\cos\Theta$ can be written in terms of the wavenumber vector $\mathbf{k} = (k, l, m)$ and its horizontal component $\mathbf{k_H} = (k, l)$ by

$$\cos\Theta = |\mathbf{k_H}|/|\mathbf{k}| \equiv \sqrt{\frac{k^2 + l^2}{k^2 + l^2 + m^2}}. \tag{14}$$

The advantage of the derivation of (13) is that it provides physical insight into the dynamics of internal waves. Specifically, the reason the frequency of shallow waves, with $\Theta \sim 90^o$, is small is because only a small component of its motion goes toward resisting gravitational forces.

2.2 The dispersion relation

An immediate consequence of the dispersion relation is that internal waves cannot propagate with frequency faster than N. The phase vector for internal waves (whose direction is perpendicular to lines of constant phase and whose magnitude is the speed of crests moving in this direction) is

$$\mathbf{c_p} \equiv \frac{\omega}{|\mathbf{k}|}\frac{\mathbf{k}}{|\mathbf{k}|} = \frac{N}{|\mathbf{k}|}\cos\Theta(\cos\phi\cos\Theta, \sin\phi\cos\Theta, \sin\Theta). \tag{15}$$

In the last of these expressions, ϕ is defined implicitly by $\tan\phi = l/k$, and represents the angle between the horizontal component of the wavenumber vector and the k-axis. Note the components of this vector is different from the phase speeds one would measure if the waves were observed at a fixed location. For example, in a vertical time series showing the passage of waves past a fixed horizontal location, the crests would move vertically at a fixed horizontal position with speed ω/m.

Another useful quantity derived from the dispersion relation is the group velocity, $\mathbf{c_g}$. This denotes the velocity at which energy is transported by the waves. Explicitly

$$\mathbf{c_g} \equiv \nabla_k\omega \equiv \left(\frac{\partial\omega}{\partial k}, \frac{\partial\omega}{\partial l}, \frac{\partial\omega}{\partial m}\right) = \frac{N}{|\mathbf{k}|}\sin\Theta(\cos\phi\sin\Theta, \sin\phi\sin\Theta, -\cos\Theta). \tag{16}$$

Thus the magnitude $|\mathbf{c_g}| = (N/|\mathbf{k}|)\sin\Theta$, which may be compared with $|\mathbf{c_p}| = (N/|\mathbf{k}|)\cos\Theta$.

An initially surprising consequence of these equations is that the group and phase velocities are orthogonal to each other and that if the wave transports energy upwards, then the phase lines move downwards, and *vice versa*.

This is seen quite explicitly in experiments in which a cylinder oscillates vertically up and down at a fixed frequency, ω, in a stratified fluid. Provided $\omega < N$, the waves propagate away from the cylinder along four beams which form a "St.

Andrews Cross" pattern with the cylinder at the center of the cross [48]. One branch of the waves emanating from the upper cylinder are revealed in the "synthetic schlieren" image shown in Fig. 3a [69]. The wavebeam emanates upward and to the right of the cylinder, transporting energy in a direction parallel to the wave crests and in the direction of $\mathbf{c_g}$. In contrast, surface waves transport energy in a direction perpendicular to the wave crests. The time series in Fig. 3b shows that, whereas the group velocity is directed upward, the crests of the waves move downward over time.

Another interesting consequence of the dispersion relation is that the vertical component of the group velocity is zero for waves with $\Theta = 0$ and $\Theta = 90^o$. The maximum vertical group velocity occurs at an intermediate angle $\Theta = \tan^{-1}(1/\sqrt{2}) \simeq 35^o$

2.3 Partial Differential Equations

Much information can be gleaned from the dispersion relation of waves. However, one must solve the equations of motion as given by a coupled set of partial differential equations in order to predict the inter-relationship between components of the velocity field and perturbation density field, and to predict energy and momentum transport by the waves.

The linearised equations of motion provide insight into the behaviour of small amplitude internal waves. For simplicity in this discussion, we neglect the effects of viscosity and we assume that the vertical variation of the background density is sufficiently long compared with the scale of the waves that we can adopt the "Boussinesq approximation": density variations are important only as they influence buoyancy forces. The Boussinesq approximation is suitable for the study of ocean, in which the density changes by less than 10% from the surface to ocean floor. In the atmosphere, the approximation is useful only over scales less than approximately 10 km [63].

If we further assume that there is no mean background flow and that the fluid is uniformly stratified (the buoyancy frequency is constant), the motion of small-amplitude internal waves is given by differential equations describing the conservation of mass assuming the fluid is incompressible, as given by (7 and (3), and the linearised form of the equations describing the conservation of momentum:

$$\begin{aligned} \rho_0 \frac{\partial u}{\partial t} &= -\frac{\partial p}{\partial x}, \\ \rho_0 \frac{\partial v}{\partial t} &= -\frac{\partial p}{\partial y}, \\ \rho_0 \frac{\partial w}{\partial t} &= -\frac{\partial p}{\partial x} - g\rho; \end{aligned} \tag{17}$$

In these equations ρ_0 is a characteristic density of the fluid.

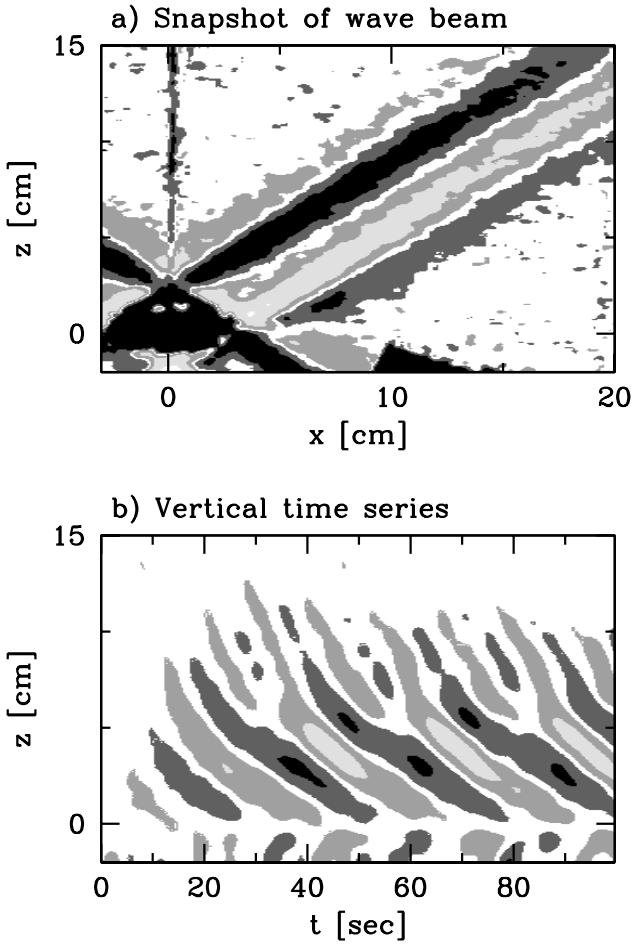

Fig. 3: a) One of the four branches of waves generated when a cylinder oscillates with frequency $\omega = 0.54\,\mathrm{s}^{-1}$ in a tank filled with uniformly stratified salt water solution whose salinity decreases with height as characterised by the buoyancy frequency $N = 1.0\,\mathrm{s}^{-1}$. The beam propagates at an angle $\sim 57^o$ to the vertical consistent with the predicted angle $\Theta = \cos^{-1}(\omega/N)$. b) Time series of the wave beams showing the evolution of the waves along a vertical slice 12.5 cm to the right of the oscillating cylinder.

These equations are conveniently rewritten in matrix form in which the nota-

tion $\partial_t \equiv \partial/\partial t$, *etc.*, is adopted:

$$\begin{pmatrix} \partial_t & 0 & 0 & 0 & \frac{1}{\rho_0}\partial_x \\ 0 & \partial_t & 0 & 0 & \frac{1}{\rho_0}\partial_y \\ 0 & 0 & \partial_t & \frac{g}{\rho_0} & \frac{1}{\rho_0}\partial_z \\ 0 & 0 & -\frac{\rho_0}{g}N^2 & \partial_t & 0 \\ \partial_x & \partial_y & \partial_z & 0 & 0 \end{pmatrix} \begin{pmatrix} u \\ v \\ w \\ \rho \\ p \end{pmatrix} = 0. \tag{18}$$

For nontrivial solutions, the determinant of the matrix in (18) must be zero. That is

$$\left[\partial_{ttt}\nabla^2 + N^2 {\nabla_H}^2 \partial_t\right] b = 0 \tag{19}$$

in which b is one of the five basic state fields (u, v, w, ρ, p), and $\nabla_H \equiv (\partial_x, \partial_y)$ is the horizontal component of the gradient operator.

Fourier transforming gives the dispersion relation for internal waves in uniformly stratified, incompressible fluid. We assume periodic solutions of the form

$$b(x, y, z, t) = A_b \exp[\imath(kx + ly + mz - \omega t)], \tag{20}$$

in which it is understood that the actual wave structure is given by the real part of b. Substituting (20) in (19) gives $-\imath\omega^3|\mathbf{k}|^2 + N^2\imath\omega|\mathbf{k_H}|^2 = 0$. Taking only non-stationary solutions, we find

$$\omega^2 = N^2 \frac{|\mathbf{k_H}|^2}{|\mathbf{k}|^2},$$

which is exactly the dispersion relation given by (13) and (14).

Effectively, the dispersion relation is an eigenvalue of the differential matrix problem (18). The corresponding eigenvectors give the inter-relationship between the basic state fields. For wave theory in general, these are known as the "polarisation relations".

Defining the vertical displacement field ξ implicitly through the relation $w = \partial\xi/\partial t$, the amplitude of the eigenfunctions, A_b, can each written in terms of the the amplitude of the vertical displacement field A_ξ. These are listed in Table 1.

Immediately apparent from the table is that the horizontal and vertical velocity fields are in phase with each other. Thus fluid parcels undergo linear (rather than circular) oscillatory motion due to waves. This is consistent with the assumption made above in deriving the dispersion relation from a parcel argument.

The vertical transport of horizontal momentum per unit mass in the x-direction is the cross-correlation, $\langle uw \rangle$, between the u and w fields. It is found by taking the average over one period of oscillation of the product between the real parts of the

Table 1: Polarisation relation and physically relevant correlations between basic state fields for small-amplitude Boussinesq internal waves in the (x,z) plane with no background rotation. As well as the basic state fields, the table lists values of the streamfunction (ψ), vorticity (ζ), the change in the squared buoyancy frequency due to stretching of isopycnals by waves (ΔN^2) and its time derivative ($N^2{}_t$). Each field b is characterised by the magnitude and phase of its complex amplitude A_b.

Defining equation	Relation to vertical displacement	
Vertical displacement: ξ	complex amplitude: A_ξ	
$\rho = -\frac{d\overline{\rho}}{dz}\xi$	$A_\rho = (-d\overline{\rho}/dz)A_\xi$	$= \frac{\rho_0}{g}N^2 A_\xi$
$\mathbf{u} = \nabla\times(\psi\hat{\mathbf{y}})$	$A_\psi = -\frac{\omega}{k}A_\xi$	$= -\frac{N}{k}\cos\Theta A_\xi$
$w = \frac{\partial\xi}{\partial t}$	$A_w = -\imath\omega A_\xi$	$= -\imath N\cos\Theta A_\xi$
$u = -\frac{\partial\psi}{\partial z}$	$A_u = \imath\frac{m\omega}{k}A_\xi$	$= \imath N\sin\Theta A_\xi$
$\zeta = -\nabla^2\psi$	$A_\zeta = -\frac{\omega}{k}\lvert\mathbf{k}\rvert^2 A_\xi$	$= -Nk\sec\Theta A_\xi$
$\Delta N^2 = -\frac{g}{\rho_0}\frac{\partial\rho}{\partial z}$	$A_{\Delta N^2} = -mN^2 A_\xi$	$= -\imath N^2 k\tan\Theta A_\xi$
$N^2{}_t = \frac{\partial\Delta N^2}{\partial t}$	$A_{N^2{}_t} = m\omega N^2 A_\xi$	$= -N^3 k\sin\Theta A_\xi$
Momentum transport	$\rho_0\langle uw\rangle = \frac{1}{4}\rho_0 N^2\sin 2\Theta\lvert A_\xi\rvert^2$	
Wave-induced mean flow	$-\langle\zeta\xi\rangle = \frac{1}{2}Nk\sec\Theta\lvert A_\xi\rvert^2$	

two fields. This can be done either by integrating in time ($\frac{1}{T}\int_0^T \mathrm{Re}(u)\mathrm{Re}(w)\,dt$), in space ($\frac{1}{\lambda_x}\int_0^{\lambda_x}\mathrm{Re}(u)\mathrm{Re}(w)\,dx$), or in phase, by setting $\phi = \mathbf{k}\cdot\mathbf{x} - \omega t$:

$$\begin{aligned}
\langle uw\rangle &\equiv \frac{1}{2\pi}\int_0^{2\pi}\mathrm{Re}\left(A_u e^{\imath\phi}\right)\mathrm{Re}\left(A_w e^{\imath\phi}\right)\,d\phi \\
&\equiv \frac{1}{2\pi}\int_0^{2\pi}\left[\frac{1}{2}\left(A_u e^{\imath\phi} + A_u{}^\star e^{-\imath\phi}\right)\right]\left[\frac{1}{2}\left(A_w e^{\imath\phi} + A_w{}^\star e^{-\imath\phi}\right)\right] \\
&\equiv \frac{1}{2}\mathrm{Re}\left(A_u A_w{}^\star\right) \\
&= \frac{1}{4}N^2\sin 2\Theta\lvert A_\xi\rvert^2. \qquad (21)
\end{aligned}$$

Here, the star denotes the complex conjugate. Thus waves with $\Theta = 0$ or $\Theta = 90^o$ transport no vertical momentum. For waves with the same value of the maximum

vertical displacement, A_ξ, those with $\Theta = 45^o$ transport the greatest momentum.

Another consequence of the polarisation relations is that the density field is $\pi/2$ out of phase with the velocity fields. Thus internal waves transport momentum but not mass. This is shown explicitly by following the same mathematical procedure as that used in deriving (21): the vertical transport of mass is given by

$$\langle \rho w \rangle \equiv \frac{1}{2}\mathrm{Re}\,(A_\rho A_w{}^\star) = 0. \tag{22}$$

Another useful quantity, particularly for the study of finite-amplitude waves, is the wave-induced mean flow. For surface waves, this is also known as "Stokes drift" and denotes the steady unidirectional flow of water in the direction of wave propagation. This current, which is typically much smaller than the phase speed of the waves, is proportional to the square of the wave amplitude. In the recent study of Hamiltonian fluid dynamics, the wave-induced mean flow is known more generally as the "pseudomomentum" [2, 60].

For internal waves the wave-induced mean flow, for example in the x-direction, is given explicitly in terms of the cross-correlation between the vertical displacement field (ξ) and the y-component ($\hat{\mathbf{y}} = \hat{\mathbf{z}}\times\hat{\mathbf{x}}$) of the vorticity field, $\zeta = (\nabla\times\mathbf{u})\cdot\hat{\mathbf{y}}$ [59, 64]

$$-\langle \zeta\xi \rangle \equiv \frac{1}{2}\mathrm{Re}\,(A_\zeta A_\xi{}^\star) = \frac{1}{2}Nk\sec\Theta|A_\xi|^2 \tag{23}$$

2.4 Ray theory

The effect upon wave propagation of non-uniform background flow $\overline{U}(z)$ and non-uniform stratification $N^2(z)$ can be described in an analytic theory provided the background varies vertically on scales much larger than the vertical extent of the waves. The mathematics are simplified in this limit by employing the "WKB" (or sometimes the "WKBJ", or sometimes the "Liouville-Green") approximation [34]. (The first to study this problem were Liouville [37] and Green [21], but later their results were independently rederived.)

Without derivation, the salient result is given here for waves propagating in the (x, z) plane. The path of the waves, as described by the function $z(x)$, is given by solving the differential equation

$$\frac{dz}{dx} = \frac{c_{gz}}{c_{gx} + \overline{U}} \tag{24}$$

In which the components of the group velocity are given by (16).

A key to anticipating the form of solutions of (24) is to realise that, due to the horizontal spatial invariance of the equations of motion and their boundary

conditions, the horizontal wavenumber, k, does not change following the motion of the waves, a consequence of Fourier series analysis. Likewise, temporal invariance implies that the absolute frequency, ω, (the frequency observed at a fixed point in space, otherwise called the "intrinsic frequency") of the waves do not change, although the relative frequency (the frequency observed moving with the background flow, otherwise called the "extrinsic frequency" or, more commonly, the "Doppler-shifted frequency") may change as the wavepacket propagates in shear flow.

In two particularly well studied cases one assumes that N^2 is constant and U varies linearly with height as $U(z) = sz$ (a uniform shear flow). Suppose that an internal wave packet is situated initially at the origin and moves upward and to the right. In the case with $s > 0$, one finds that the wavepacket asymptotically approaches a vertical level z_c where the background flow speed, $\overline{U}(z_c)$, equals the wavepacket's constant horizontal phase speed, ω/k. A straightforward calculation reveals

$$z_c = \frac{N}{sk} \cos\Theta. \tag{25}$$

This height is known as the "critical level". A more detailed analysis reveals that as waves approach the critical level, their amplitude increases until the waves overturn and break. Thus a background flow, such as the jet stream in the atmosphere, can act to shield the upper level flow from waves. Near the critical level breaking waves deposit momentum to the mean flow and thus locally accelerate the fluid, which further shields the upper level from waves. A dramatic example of these dynamics are manifest in laboratory experiment that models the quasi-biennial oscillation in the equatorial stratosphere [58].

Present-day models of the general circulation of the Earth's atmosphere employ heuristic schemes based, in part, upon the above remarks in order to include the effects of drag upon the atmosphere by internal waves that originate from mountainous terrain and which break near critical levels in the middle and upper atmosphere [36, 54, 43].

Though successful in enabling the models to predict more realistic wind speeds, recent work suggests this heuristic approach is too simplistic. For example, Shutts [61, 62] has shown that waves can pass through a critical level if the flow speed veers with height (that is, if we relax the constraint that the flow moves only in the x-direction and instead, for example, allow the flow to blow increasingly in the y-direction at increasing vertical levels).

Ray theory has garnered renewed interest recently in the study of small-scale internal waves that are refracted by a spectrum of large-scale, slow frequency internal waves, which effectively impose a time-varying background mean flow [19, 7, 8, 6, 10]. A significant consequence of this work is to show that critical

levels may not pose a barrier to transport by waves if the shear is time dependent. Continuing research may help to explain, for example, the observed spectrum of internal waves in the middle atmosphere [25]).

In a second well-studied case, one considers the circumstance in which a uniformly stratified flow has uniform but negative shear ($s < 0$). In this circumstance, waves with frequency ω and horizontal wavenumber k that move upward from $z = 0$ are Doppler-shifted to increasing frequencies $\Omega = \omega - k\overline{U} = \omega - ksz$. Eventually, the waves reach a level z_r at which the Doppler-shifted frequency equals the buoyancy frequency. Explicitly

$$z_r = \frac{N}{k(-s)}(1 - \cos\Theta) \tag{26}$$

Similarly, wave reflection may occur in a fluid with uniform flow ($\overline{U} = 0$) but whose stratification weakens with height. For example, if $N^2(z) = {N_0}^2(1 - z/H)$, then

$$z_r = H(1 - \cos\Theta) \tag{27}$$

In either circumstance, one finds that the waves reflect from the level z_r and thereafter transport energy and momentum back to where they originated. When one examines the structure of the wave near the reflection level itself, one finds that the slope dz/dx becomes infinitely large, in violation with the conditions required by the WKB-approximation. At the point of reflection there are three distinct wave groups: the incident and reflected wave below z_r and an "evanescent" wave whose amplitude decreases exponentially with height above z_r. This structure is known as a "caustic" [34].

Ray theory has proven successful in reproducing the paths followed by experimentally generated internal wave beams in uniformly stratified, uniform shear flows [29] and in stationary, non-uniformly stratified fluids [70]. The latter experiments also examined the consequences of violating the WKB-approximation, showing that internal waves reflect from a level lower than z_r if N^2 decreases rapidly with height compared with the extent of the internal wave beam.

Ray theory has also proven successful in predicting the path of small-amplitude internal wave groups in uniform shear as measured from fully nonlinear numerical simulations [66]. However, as discussed in section 4, the theory breaks down for waves with amplitudes as small as 1 percent of the horizontal wavelength.

2.5 Anelastic effects

To this point we have considered small-amplitude wave propagation as described within the limits of the Boussinesq approximation. If we consider the

propagation of waves in the atmosphere (the density of which decreases in height by approximately 1/2 every 6 km), it is necessary to relax the constraint that density variations are significant only in the buoyancy term of the equations of motion. Instead we allow $\rho_{\rm T} \to \overline{\rho}$ in (6), This is the "anelastic approximation".

Thermodynamics play an important role for atmospheric waves in general. As air moves up and down the fluid is heated and cooled, respectively, and so the density of fluid parcels vary. A quantity that characterises these effects is the potential temperature:

$$\theta = T\left(\frac{p}{p_0}\right)^{-2/7} \tag{28}$$

The derivation of (28) can be found in any standard textbook on dynamic meteorology (*e.g.* see Gill [20] §3.7). Here T and p are the temperature and pressure of a fluid parcel at some vertical level and p_0 is a reference value of pressure, typically taken to be $p_0 = 1000\,$millibars, the pressure at sea level. Physically, θ represents the temperature a fluid parcel would have if brought adiabatically to sea level. This is a particularly useful quantity because it is conserved following the adiabatic motion of a fluid parcel. Note that while the temperature in the lower atmosphere decreases with height, the potential temperature generally increases with height.

In the anelastic approximation, the squared buoyancy frequency is defined in term of the background potential temperature, $\overline{\theta}(z)$, by

$$N^2 = \frac{g}{\overline{\theta}}\frac{d\overline{\theta}}{dz}. \tag{29}$$

There are two main differences between this definition and that given by (10): $\overline{\theta}$ rather than a constant reference value, θ_0, appears in the denominator of the fraction before the derivative, and there is no negative sign on the right-hand side of the definition. The latter is consistent with the observation that in a stable (non-convective) atmosphere, potential temperature increases with height. Thus N^2 as given by (29) is generally positive.

Here we study the simplest circumstance of an isothermal atmosphere (whose temperature T_c is independent of height) with no mean flow. In this case, thermodynamics and hydrostatic balance dictates that the background pressure and density are proportional to $\exp(-z/H_s)$ where $H_s = RT_c/g$ is called the "scale-height" ($\simeq 8.4\,$km in the atmosphere using the value of the ideal gas constant R). One finds that the corresponding background potential temperature is $\overline{\theta} = \theta_0 \exp[\frac{2}{7}(z/H)]$ and $N^2 = (2/7)g/H_s$.

The partial differential equations describing the motion of small-amplitude

internal waves is given, in matrix form, by

$$\begin{pmatrix} \partial_t & 0 & 0 & 0 & \frac{1}{\overline{\rho}}\partial_x \\ 0 & \partial_t & 0 & 0 & \frac{1}{\overline{\rho}}\partial_y \\ 0 & 0 & \partial_t & \frac{g}{\overline{\rho}} & \frac{1}{\overline{\rho}}\partial_z \\ 0 & 0 & -\overline{\rho}/gN^2 & \partial_t & 0 \\ \partial_x & \partial_y & \partial_z & 0 & 0 \end{pmatrix} \begin{pmatrix} u \\ v \\ w \\ \rho \\ p \end{pmatrix} = 0. \tag{30}$$

As waves propagate upward they transport momentum, the magnitude of which, according to (21), is proportional to the squared amplitude of the waves. Because the density of the atmosphere decreases with height, the waves must increase in amplitude with height in order to conserve momentum. Hence we assume solutions of the form

$$f(x, y, z, t) = f_0 \exp(\imath(\mathbf{k} \cdot \mathbf{x} - \omega t)] \exp(z/2H), \tag{31}$$

and substitute into (30).

The resulting matrix eigenvalue problem gives the dispersion relation for anelastic waves:

$$\omega^2 = N^2 \frac{|\mathbf{k_H}|^2}{|\mathbf{k}|^2 + \Gamma^2}, \tag{32}$$

in which $\Gamma = (3/14){H_s}^{-1}$. In the limit $H_s \to \infty$, (32) is identical to the dispersion relation for Boussinesq waves, (13).

The significant difference in the dynamics is in the wave structure, as given by (31). In reality, the waves do not grow in amplitude indefinitely, but ultimately they overturn and break. As well as critical-level absorption, discussed in §2.4, this is the second well-studied mechanism for wave breaking and deposition of momentum to the mean flow in the atmosphere.

2.6 Background rotation effects

For internal waves that evolve on time scales comparable to the rotational period of the Earth, it is also important to include the effect of Coriolis forces. For simplicity, we return here to the Boussinesq approximation and write the resulting equations of motion in matrix form by

$$\begin{pmatrix} \partial_t & -f & 0 & 0 & \frac{1}{\rho_0}\partial_x \\ f & \partial_t & 0 & 0 & \frac{1}{\rho_0}\partial_y \\ 0 & 0 & \partial_t & \frac{g}{\rho_0} & \frac{1}{\rho_0}\partial_z \\ 0 & 0 & -\frac{\rho_0}{g}N^2 & \partial_t & 0 \\ \partial_x & \partial_y & \partial_z & 0 & 0 \end{pmatrix} \begin{pmatrix} u \\ v \\ w \\ \rho \\ p \end{pmatrix} = 0 \tag{33}$$

Here the constant $f = 2\Omega \sin\phi_0$ is the Coriolis parameter, which depends upon the rotational frequency of the Earth ($\Omega = 2\pi/(1\,\text{day})$) and the local latitude ϕ_0. (At the North Pole, $\phi_0 = 90^o$ and so $f = 2\Omega$.) The parameter f is sometimes called the "inertial frequency" because gravity has negligible affect upon fluid parcels moving near this frequency and thus they move only under their own inertia. In the atmosphere and oceans at mid-latitudes, $f \simeq 10^{-4}\text{s}^{-1}$, two orders of magnitude smaller than typical values of N.

Assuming plane wave solutions of the form (20) the matrix eigenvalue problem gives the dispersion relation

$$\omega^2 = N^2 \cos^2\Theta + f^2 \sin^2\Theta \tag{34}$$

where Θ is again defined by (14).

Obviously, in the case $f = 0$ we recover (13). Equation (34) shows that f is a low-frequency cut-off: internal waves cannot propagate with frequencies lower than f. Internal waves with frequency close to f are called "inertia-gravity waves".

The phase lines of inertia-gravity waves waves are almost horizontal ($\Theta \sim 90^o$). A study of the corresponding polarisation relations reveal that the u and v fields are 90^o out of phase implying that fluid parcels prescribe near-horizontal elliptical paths during the passage of the waves.

Measurements of internal waves in the atmosphere have revealed that most of their energy spectrum is contained near inertial frequencies. For this reason, and also because only recently large-scale atmospheric simulations have been able to resolve the spatial structure of inertia-gravity waves, there have been numerous theoretical and numerical studies have been performed to examine their dynamics [15, 33]. However, because the waves are necessarily long period and exist typically over long scales, simplified models which assume stationary background flows are of questionable realistic value.

3 Weakly Nonlinear Theory

In the preceding section it is assumed throughout that the waves are of small amplitude. This is a useful approximation because the analytic solutions of the resulting linearised equations can be found for a wide variety of circumstances.

Weakly nonlinear theory describes the dynamics of waves with amplitudes that are non-negligible but still sufficiently small that analytic solutions can be found through perturbation theory. Typically, weakly nonlinear dynamics involve wave-wave interactions, for which the superposition principle breaks down, and interactions between waves and the wave-induced mean flow.

Although a great deal of work has examined the weakly nonlinear dynamics of water waves [56, 24, 3] relatively little research has gone into studying the corresponding internal wave dynamics.

3.1 Modulational instability

Weakly nonlinear dynamics act to modify the dispersion relation for waves:

$$\omega_{\rm wnl} = \omega(\mathbf{k}) + \omega_2(\mathbf{k})A^2, \tag{35}$$

in which the first term on the right-hand side of the equations is the dispersion relation determined from linear theory (*e.g.* equation (13)). Considering for now the motion in the x-direction, a periodic wave train is said to be "modulationally stable" (remaining periodic for all time) if [76, 77]

$$\omega_2 \frac{\partial^2 \omega}{\partial k^2} > 0 \tag{36}$$

Indeed, for deep water waves it has been shown that the waves are always modulationally unstable, even for water waves of infinitessimally small amplitude. However, because the growth rate of the instability is proportional to amplitude, in realistic circumstances it is unlikely to manifest itself during the life-cycle of very small amplitude waves. The structure of this instability was described by Benjamin and Feir [3] who showed that the energy in the spectrum repeatedly transfers to different "sideband" wavenumbers and then transfers back to the original wavenumber following what is known more generally as the Fermi-Pasta-Ulam (FPU) recurrence phenomena [16].

The modulational stability of Boussinesq, non-rotating internal waves has been examined analytically by Grimshaw [23] and both analytically and numerically by Sutherland [67]. The latter has shown that the criterion (36) predicts that horizontally periodic, vertically compact internal waves are modulationally unstable to the growth of vertical sideband wavenumbers if their frequency is higher than that of the waves with the fastest vertical group velocity, that is, if

$$\Theta < \Theta_c = \tan^{-1}(2^{-1/2}) \simeq 35^o. \tag{37}$$

Indeed fully nonlinear numerical simulations show the emergence of FPU recurrence for these waves and show that waves with $\Theta > \Theta_c$ remain modulationally stable. Horizontally compact internal waves are predicted to be modulationally unstable to the growth of horizontal sideband wavenumbers if $\Theta > \Theta_c = \sin^{-1}(2^{-1/3}) \simeq 53^o$.

3.2 Wave-wave interactions

Modulational instability does not imply wave breaking, only non-steadiness of a periodic wavetrain. However, other weakly nonlinear dynamics result in overturning and breaking waves.

In general, three waves of wavenumber vector $\mathbf{k}_i$ and frequencies ω_i, for $i = 1, 2, 3$, may interact in what is called a "resonant triad" if $\mathbf{k}_3 = \mathbf{k}_1 \pm \mathbf{k}_2$ and $\omega_3 = \omega_1 \pm \omega_2$ (*e.g.*, see Phillips [57]). This amounts to requiring $\cos\Theta_3 = \cos\Theta_1 \pm \cos\Theta_2$, in which Θ_i is given by (14). In practise three possible resonant couplings are of interest: under "elastic scattering", energy in a high frequency wave is transported to another with nearly equal and opposite wavenumber vector; under "induced diffusion", energy in a low frequency wave is transported to a high frequency wave; under "parametric subharmonic instability", energy is extracted from a low wavenumber mode and deposited into to high frequency waves with nearly equal and opposite wavenumbers.

Observations of internal waves in the ocean suggest that elastic scattering and induced diffusion both play an important role in governing the energy spectrum of waves in the ocean interior. Both mechanisms act on time scales comparable to one wave period [50].

For internal waves that are periodic everywhere in space, internal waves are found to be parametrically unstable even at infinitessimally small amplitudes [28, 38]. The instability grows through resonant coupling between the initial waves and their superharmonics (whose horizontal wavenumbers are an integer multiple of the initial waves). Through this coupling, the superharmonic waves extract energy from the initial waves and grow in amplitude until ultimately they break.

Though mathematically interesting, the study is not relevant to realistic circumstances for two reasons. First, typical instability growth rates are so small that parametric instabilities would not likely develop significantly between the time that the waves are generated and when they break. Second, parametric instability is the dominant mode of instability only in the case of plane-periodic waves. Localised internal wavepacket dynamics have been found to be governed dominantly due to interactions between the waves and the wave-induced mean flow [67].

3.3 Breaking instabilities

Internal waves become unstable and break if their amplitude is sufficiently large. Linear theory predicts overturning occurs if the amplitude is so large that $\partial\rho_{\rm T}/\partial t \equiv d\overline{\rho}/dz + \partial\rho/\partial z > 1$ somewhere in the flow field. Using the polarisation relations in Table 1, the "overturning condition" can be derived. This states that waves propagating at angle Θ to the vertical are unstable if the amplitude A_ξ of the vertical displacement field exceeds $A_{\rm OT}$ where

$$A_{\rm OT} = \frac{1}{2\pi}\cot\Theta. \tag{38}$$

Due to interactions between waves and the wave-induced mean flow, simulations show that internal waves in fact are unstable at much smaller amplitudes

unless Θ is close to 90^o. The criterion for instability is called the "self-acceleration" condition, which states that the waves become unstable if the wave-induced mean flow exceeds the horizontal group velocity. Using (16) and (23), it is apparent that the waves are unstable if

$$A_\xi > A_{\rm SA} \equiv \frac{\lambda_x}{2\pi\sqrt{2}} \sin 2\Theta, \tag{39}$$

in which $\lambda_x = 2\pi/k$ is the horizontal wavelength. Thus waves with $\Theta \simeq 0$ ($\omega \simeq N$) are unstable to overturning and breaking even at infinitessimally small amplitudes. Even for the most stable waves, with $\Theta = 45^o$, the waves are unstable if their amplitude is larger than 11% of the horizontal wavelength. Numerical simulations show that the onset of instability is rapid, occurring within 5 buoyancy periods, $2\pi/N$.

3.4 Critical Level absorption

Weakly nonlinear models for internal waves in stratified shear flow have been examined by a number of authors [40, 41, 12, 31], there emphasis being on examining the flows whose basic states are near the marginal stability boundary; that is, for stratified shear flows with the minimum value of the gradient Richardson number ${\rm Ri} \equiv N^2/(\overline{U}')^2 \simeq 1/4$ [46, 26]. In a analytical-numerical study, Lamb and Pierrehumbert [31] showed that two-dimensional internal waves originating from topography underlying a critical layer could transmit through the layer, in a manner reminiscent of coherent light waves been transmitted from a resonant cavity in a laser.

3.5 Wave reflection

The interactions between waves and the wave-induced mean flow can act to allow waves to transmit well above a reflection level, z_r that would occur in linear theory when a wavepacket moves upward in a background flow with uniform but negative shear, $s < 0$. We hypothesize that this occurs because the wave-induced mean flow creates a local mean shear that counteracts the background shear. A simple calculation reveals that the positive shear associated with the wave-induced mean flow is equal to $|s|$ when

$$A_{\rm WR} = \sqrt{2\sigma_z k_x \frac{s}{N} \cos^3\Theta} \frac{N}{k}, \tag{40}$$

in which σ_z is the vertical width of the wavepacket [66].

3.6 Laboratory Experiments

At present few experiments have been performed to examine the weakly nonlinear dynamics of internal waves. Resonant interactions between short and long waves were examined analytically and experimentally by Koop and Redekopp [30]. and between equal and opposite propagating wave beams by Teoh *et al* [73]. The latter observed the generation of an evanescent disturbance in the overlapping region which consequently grew and ultimately broke.

Weakly nonlinear effects are also apparent where the upward and downward propagating wavebeams near the cylinder overlap [69, 72]. In particular, waves with double the frequency of oscillation of the cylinder have been observed in tandem with the primary wavebeams. Though this could be due to wave-wave interactions, tracking the origin of the secondary beams to the cylinder itself implies that the beams are created due to interactions between the waves and the viscous boundary layer surrounding the cylinder.

4 Nonlinear Theory

Unlike linear and weakly nonlinear theories, the dynamics of fully nonlinear finite-amplitude internal waves, with very few and trivial exceptions, can be examined only through analysis of numerical simulations in which the Navier-Stokes equations are iteratively solved in time.

4.1 Wave modulation

The propagation of two-dimensional finite-amplitude, Boussinesq internal waves in stationary, uniformly stratified fluid has been examined by Sutherland [67]. This study both confirmed the validity of the modulational stability criterion (37) as well as the self-acceleration condition (39). The latter was shown to be successful in predicting the stability to breaking of horizontally periodic, vertically compact wavepackets. Horizontally and vertically compact wavepackets were found to be stable at moderately larger amplitudes than predicted however, particularly for waves with small Θ.

4.2 Critical level absorption

At a critical level, z_c, ray theory predicts the waves approaching from below should break and be absorbed by the mean flow. However, as finite-amplitude waves approach a critical level, one finds that the wavepackets may be partially transmitted across z_c or partial reflect below z_c.

Recently, computer speeds and memory have increased enough to run high-

resolution numerical simulations of internal waves incident upon a critical level [5, 78, 79, 14]. The simulations show that the breaking occurs due to convective overturning modified by shear. The instability is inherently three-dimensional. The incident wave energy is ultimately partitioned into a three main proportions associated with 1) acceleration of the mean flow, 2) irreversible mixing of the local stratification, and 3) a reflected wave packet. In their study of three-dimensional waves, Winters and d'Asaro [79] showed that the proportion of the wavepacket that deposits energy to the mean flow is sensitive to the wave amplitude and the relative strength of the shear at the critical level.

4.3 Wave reflection

The nonlinear dynamics of finite-amplitude internal waves incident upon a reflecting level has been studied for the case of two-dimensional, Boussinesq waves. Sutherland [64] examined the dynamics of waves in a stationary background fluid whose buoyancy frequency decreased from one constant value to another constant value over a short vertical distance. A related study examined the reflection of waves in a uniformly stratified fluid in a background flow that decreased from one constant value to another over a short distance [65]. In both cases it was found that a greater proportion of the incident wavepacket was transmitted across the reflecting level if the waves were of large amplitude. Even if no reflecting level existed, a larger proportion of finite-amplitude waves were found to reflect from the varying region of the background wind or stratification. Both nonlinear phenomena occurred because the wave-induced mean flow Doppler-shifted the frequency of the incident waves.

The dynamics of finite-amplitude Boussinesq internal waves in a uniform shear flow were examined by Sutherland [66]. Surprisingly this study revealed that horizontally and vertically compact wavepackets may propagate well beyond a reflection level at an approximately constant vertical speed. The results were consistent with the transmission condition (40).

5 Conclusions

Though much is understood about the dynamics of small-amplitude waves, a great deal is unknown about the propagation of finite-amplitude internal waves. Some specific outstanding problems are listed here.

- Conditions for modulational instability and breaking due to self-acceleration have not yet been derived for anelastic waves or inertia-gravity waves.

- The transmission condition has been derived and tested for waves in a uniformly stratified shear flow. No such test has yet been performed for waves

in a uniform flow with decreasing stratification with height.

- Though some fully nonlinear simulations of two-dimensional non-hydrostatic waves have been performed, their three-dimensional counterparts remain to be examined. In particular, it would be interesting to study finite-amplitude effects as wavepackets approach a critical level in a veering wind.

- Large-eddy simulations (LES) model the interactions of waves near a critical layer without resolving the breaking in detail [54, 43, 49]. The emphasis of these studies is to evaluate whether heuristic parameterisations of wave breaking can indeed account for discrepancies between observed flow speeds and those predicted by models that ignore the effect of internal waves. Though such parameterisations have been successful in improving model predictions, the results of high-resolution simulations imply that the heuristic methods employed are not always trustworthy. Future research should attempt to bring LES and high resolution approaches together in a way that allows for speedy but reliable parameterisations of breaking waves.

- Few laboratory experiments have been performed to examine finite amplitude effects, in part because probes give amplitude measurements at a point and classical schlieren visualisation methods [47] reveal phase but not amplitude information. Using the recently developed "synthetic schlieren" method, one can measure amplitudes of a two-dimensional wave field everywhere in space and time [13]. Further experimental progress will be made with the ongoing extension of this technique to measure three-dimensional wave fields [17].

This review mentions only briefly here other significant and active research areas in internal wave theory, including their interaction with rigid boundaries ([74, 4]) and turbulence ([32, 27, 53]), and their generation by flow over topography ([55]), convection ([1]), shear instability ([35, 42, 44, 18, 68, 71]) and geostrophic adjustment ([39]).

The focus here has been on internal waves in a continuously stratified fluid, the assumption being that the vertical extent of the stratified fluid is significantly longer than the vertical extent of the wavepackets. Nonetheless, in many natural circumstances internal waves are manifest at the interface between two fluids of different (but comparable) density. With the realization that such large-amplitude waves occur in the atmosphere (*e.g.* at atmospheric inversions in the form of Australia's Morning Glory [11, 45]) and ocean (*e.g.* at the thermocline and generated by tidal flow over the continental shelf ([51, 52]), the mathematics of solitary waves have been brought to bear upon these problems [22].

Bibliography

[1]M. J. Alexander. A simulated spectrum of convectively generated gravity waves: Propagation from the tropopause to the mesopause and effects on the middle atmosphere. *J. Geophys. Res.* 101: 1571–1588 (1996).

[2]D. G. Andrews and M. E. McIntyre. An exact theory of nonlinear waves on a Lagrangian-mean flow. *J. Fluid Mech.* 89: 609–646 (1978).

[3]T. B. Benjamin and J. E. Feir. The disintegration of wavetrains on deep water. *J. Fluid Mech.* 27: 417–430 (1967).

[4]P. Bouruet-Aubertot, J. Sommeria, and C. Staquet. Instabilities and breaking of standing internal gravity waves. *J. Fluid Mech.* 285: 265–301 (1995).

[5]R. J. Breeding. A nonlinear model of the break-up of internal gravity waves due to their exponential growth with height. *J. Geophys. Res.* 77: 2681–2692 (1972).

[6]D. Broutman, C. Macaskill, M. E. McIntyre, and J. W. Rottman. On Doppler-spreading models of internal waves. *Geophys. Res. Lett.* 24: 2813–2816 (1997).

[7]D. Broutman and W. R. Young. On the interaction of small-scale oceanic internal waves with near-inertial waves. *J. Fluid Mech.* 166: 341–358 (1986).

[8]D. L. Bruhwiler and T. J. Kaper. Wavenumber transport: Scattering of small-scale internal waves by large-scale wavepackets. *J. Fluid Mech.* 289: 379–405 (1995).

[9]D. Brunt. The period of simple vertical oscillations in the atmosphere. *Quart. J. Roy. Meteorol. Soc.* 53: 30–32 (1927).

[10]G. Buckley, D. Broutman, J. W. Rottman, and S. Eckermann. On the importance of weak steady shear in the refraction of short internal waves. *Geophys. Res. Lett.* 26: 2877–2880 (1999).

[11]D. R. Christie, K. J. Muirhead, and A. L. Hales. Intrusive density flows in the lower troposphere: a source of atmospheric solitons. *J. Geophys. Res.* 84: 4959–4970 (1979).

[12]S. M. Churilov and I. G. Shukhman. Nonlinear stability of a stratified shear flow: a viscous critical layer. *J. Fluid Mech.* 180: 1–20 (1987).

[13]S. B. Dalziel, G. O. Hughes, and B. R. Sutherland. Whole field density measurements. *Experiments in Fluids* 28: 322–335 (2000).

[14]A. Dörnbrack, T. Gerz, and U. Schumann. Turbulent breaking of overturning gravity waves below a critical level. *Appl. Sci. Res.* 54: 163–176 (1995).

[15]T. J. Dunkerton. Shear instability of internal inertia-gravity waves. *J. Atmos. Sci.* 54: 1628–1641 (1997).

[16]E. Fermi, J. Pasta, and S. Ulam. Studies of nonlinear problems I, Los Alamos Report LA 1940, 1955. In A. C. Newell, editor, *reproduced in Nonlinear Wave Motion* Amer. Math. Soc., Providence, RI (1974).

[17]M. R. Flynn, K. Onu, and B. R. Sutherland. Internal wave generation by a vertically oscillating sphere. *J. Fluid Mech.* page submitted (2001).

[18]D. C. Fritts. Shear excitation of atmospheric gravity waves. *J. Atmos. Sci.* 39: 1936–1952 (1982).

[19]D. C. Fritts. The transient critical-level interaction in a Boussinesq fluid. *J. Geophys. Res.* 87: 7997–8016 (1982b).

[20]A. E. Gill. *Atmosphere-Ocean dynamics.* Academic Press San Diego (1982).

[21]G. Green. On the motion of waves in a variable canal of small depth and width. *Trans. Cambridge Philos. Soc.* [See Mathematical Papers, pp. 223–230. Macmillan, London, 1871] (1838).

[22]R. H. J. Grimshaw. Nonlinear internal gravity waves in a slowly varying medium. *J. Fluid Mech.* 54: 193–207 (1972).

[23]R. H. J. Grimshaw. The modulation and stability of an internal gravity wave. Technical Report 32 Department of Mathematical Sciences, University of Melbourne (1975b).

[24]K. Hasselmann. On the non-linear energy transfer in a gravity wave spectrum. Part 1. *J. Fluid Mech.* 12: 481–500 (1962).

[25]C. O. Hines. The saturation of gravity waves in the middle atmosphere. Part II: Development of the Doppler-spread theory. *J. Atmos. Sci.* 48: 1360–1379 (1991).

[26]L. N. Howard. Note on a paper by John W. Miles. *J. Fluid Mech.* 10: 509–512 (1961).

[27]A. V. Ivanov, L. A. Ostrovsky, I. A. Soustova, and L.Sh. Tsimring. Interaction of internal waves and turbulence in the ocean. *Dyn. Atmos. Ocean* 7: 221–232 (1983).

[28]J. Klostermeyer. Two- and three-dimensional parametric instabilities in finite amplitude internal gravity waves. *Geophys. Astrophys. Fluid Dyn.* 64: 1–25 (1991).

[29]C. G. Koop. A preliminary investigation of the interaction of internal gravity waves with a steady shearing motion. *J. Fluid Mech.* 113: 347–386 (1981).

[30]C. G. Koop and L. G. Redekopp. The interaction of long and short internal gravity waves: Theory and experiment. *J. Fluid Mech.* 111: 367–409 (1981).

[31]K. Lamb and R. T. Pierrehumbert. Steady-state nonlinear internal gravity-wave critical layers satisfying an upper radiation condition. *J. Fluid Mech.* 238: 371–404 (1992).

[32]P. H. LeBlond. On the damping of internal gravity waves in a continuously stratified ocean. *J. Fluid Mech.* 25: 121–142 (1966).

[33]M.-Pascale Lelong and Timothy J. Dunkerton. Intertia-gravity wavebreaking in three dimensions. Part I: Convectively stable waves. *J. Atmos. Sci.* 55: 2473–2488 (1998).

[34]M. J. Lighthill. *Waves in Fluids.* Cambridge University Press Cambridge, England (1978).

[35]R. S. Lindzen. Stability of a Helmholtz velocity profile in a continuously stratified infinite Boussinesq fluid – applications to clear air turbulence. *J. Atmos. Sci.* 31: 1507–1514 (1974).

[36]R. S. Lindzen. Turbulence and stress owing to gravity wave and tidal breakdown. *J. Geophys. Res.* 86: 9707–9714 (1981).

[37]J. Liouville. Sur le développement des fonctions ou parties de fonctions en séries . . . . *J. Math. Pure Appl.* 2: 16–35 (1837).

[38]P. N. Lombard and J. J. Riley. On the breakdown into turbulence of propagating internal waves. *Dyn. Atmos. Ocean* 23: 345–355 (1996).

[39]Z. Luo and D. C. Fritts. Gravity-wave excitation by geostrophic adjustment of the jet stream. Part II: Three-dimensional forcing. *J. Atmos. Sci.* 50: 104–115 (1993).

[40]S. A. Maslowe. The generation of clear air turbulence by nonlinear waves. *Stud. App. Maths* 51: 1–16 (1972).

[41]S. A. Maslowe. Critical layers in shear flows. *Ann. Rev. Fluid Mech.* 18: 405–432 (1986).

[42]G. Mastrantonio, F. Einaudi, D. Fua, and D. P. Lalas. Generation of gravity waves by jet streams in the atmosphere. *J. Atmos. Sci.* 33: 1730–1738 (1976).

[43]N. A. McFarlane. The effect of orographically excited gravity wave drag on the general circulation of the lower stratosphere and troposphere. *J. Atmos. Sci.* 44: 1775–1800 (1987).

[44]M. E. McIntyre and M. A. Weissman. On radiating instabilities and resonant overreflection. *J. Atmos. Sci.* 35: 1190–1196 (1978).

[45]A. Menhofer, R. K. Smith, M. J. Reeder, and D. R. Christie. "Morning-Glory" disturbances and the environment in which they propagate. *J. Atmos. Sci.* 54: 1712–1725 (1997).

[46]J. W. Miles. On the stability of heterogeneous shear flows. *J. Fluid Mech.* 10: 496–508 (1961).

[47]D. E. Mowbray. The use of schlieren and shadowgraph techniques in the study of flow patterns in density stratified liquids. *J. Fluid Mech.* 27: 595–608 (1967).

[48]D. E. Mowbray and B. S. H. Rarity. A theoretical and experimental investigation of the phase configuration of internal waves of small amplitude in a density stratified liquid. *J. Fluid Mech.* 28: 1–16 (1967a).

[49]J. Muench and E. Kunze. Internal wave interactions with equatorial deep jets. Part II. acceleration of the jets. *J. Phys. Oceanogr.* 30: 2099–2110 (2000).

[50]W. Munk. Internal wave and small-scale processes. In B. A. Warren and C. Wunsch, editors, *Evolution of Physical Oceanography* 264–291, MIT Press, Cambridge, MA (1981).

[51]A. R. Osborne and T. L. Burch. Internal solitons in the Andaman Sea. *Science* 208: 451–460 (1980).

[52]L. A. Ostrovsky and Yu. A. Stepanyants. Do internal solitons exist in the ocean? *Rev. Geophys.* 27: 293–310 (1989).

[53]L. A. Ostrovsky and D. V. Zaborskikh. Damping of internal gravity waves by small-scale turbulence. *J. Phys. Oceanogr.* 26: 388–397 (1996).

[54]T. N. Palmer, G. J. Shutts, and R. Swinbank. Alleviation of a systematic westerly bias in general circulation and numerical weather prediction models through an orographic gravity drag parametrization. *Quart. J. Roy. Meteor. Soc.* 112: 1001–1039 (1986).

[55]W. R. Peltier and T. L. Clark. The evolution and stability of finite-amplitude mountain waves. Part II: Surface wave drag and severe downslope windstorms. *J. Atmos. Sci.* 36: 1498–1529 (1979).

[56]O. M. Phillips. On the dynamics of unsteady gravity waves of finite amplitude. Part 1. The elementary interactions. *J. Fluid Mech.* 9: 193–217 (1960).

[57]O. M. Phillips. *The Dynamics of the Upper Ocean.* Cambridge University Press Cambridge 2nd edition (1966).

[58]R. A. Plumb and A. D. McEwan. The instability of a forced standing wave in a viscous, stratified fluid: A laboratory analogue of the quasi-biennial oscillation. *J. Atmos. Sci.* 35: 1827–1839 (1978).

[59]J. F. Scinocca and T. G. Shepherd. Nonlinear wave-activity conservation laws and Hamiltonian structure for the two-dimensional anelastic equations. *J. Atmos. Sci.* 49: 5–27 (1992).

[60]T. G. Shepherd. Symmetries, conservation laws, and Hamiltonian structure in geophysical fluid dynamics. *Adv. Geophys.* 32: 287–338 (1990).

[61]G. J. Shutts. Gravity-wave drag parametrization over complex terrain: the effect of critical level absorption in directional wind shear. *Quart. J. Roy. Meteorol. Soc.* 121: 1005–1021 (1995).

[62]G. J. Shutts. Stationary gravity-wave structure in flows with directional wind shear. *Quart. J. Roy. Meteorol. Soc.* 124: 1421–1442 (1998).

[63]E. A. Spiegel and G. Veronis. On the Boussinesq approximation for a compressible fluid. *Astrophys. J.* 131: 442–447 (1960).

[64]B. R. Sutherland. Internal gravity wave radiation into weakly stratified fluid. *Phys. Fluids* 8: 430–441 (1996).

[65]B. R. Sutherland. Propagation and reflection of large amplitude internal gravity waves. *Phys. Fluids* 11: 1081–1090 (1999).

[66]B. R. Sutherland. Internal wave reflection in uniform shear. *Q.J.R.M.S.* 126: 3255–3287 (2000).

[67]B. R. Sutherland. Finite-amplitude internal wavepacket dispersion and breaking. *J. Fluid Mech.* 429: 343–380 (2001).

[68]B. R. Sutherland, C. P. Caulfield, and W. R. Peltier. Internal wave generation and hydrodynamic instability. *J. Atmos. Sci.* 51: 3261–3280 (1994).

[69]B. R. Sutherland, S. B. Dalziel, G. O. Hughes, and P. F. Linden. Visualisation and measurement of internal waves by "synthetic schlieren". Part 1: Vertically oscillating cylinder. *J. Fluid Mech.* 390: 93–126 (1999).

[70]B. R. Sutherland, G. O. Hughes, S. B. Dalziel, and P. F. Linden. Internal waves revisited. *Dyn. Atmos. Ocean* 31: 209–232 (2000).

[71]B. R. Sutherland and P. F. Linden. Internal wave generation by flow over a thin barrier. *J. Fluid Mech.* 377: 223–252 (1998).

[72]B. R. Sutherland and P. F. Linden. Internal wave excitation by a vertically oscillating elliptical cylinder. *Phys. Fluids* page submitted (2001).

[73]S. G. Teoh, G. N. Ivey, and J. Imberger. Laboratory study of the interaction between two internal wave rays. *J. Fluid Mech.* 336: 91–122 (1997).

[74]S. A. Thorpe. The generation of alongslope currents by breaking internal waves. *J. Phys. Oceanogr.* 29: 29–38 (1999).

[75]V. Väisälä. " Uber die wirkung der windschwankungen auf die pilotbeobachtungen. *Soc. Sci. Fenn. Commentat. Phys.-Math.* 2: 19–37 (1925).

[76]G. B. Whitham. A general approach to linear and nonlinear dispersive waves using a Lagrangian. *J. Fluid. Mech.* 22: 273–283 (1965).

[77]G. B. Whitham. *Linear and Nonlinear Waves.* John Wiley and Sons, Inc. New York (1974).

[78]K. B. Winters and E. A. D'Asaro. Two-dimensional instability of finite amplitude internal gravity wave packets near a critical level. *J. Geophys. Res.* 94: 12709–12719 (1989).

[79]K. B. Winters and E. A. D'Asaro. Three-dimensional wave instability near a critical level. *J. Fluid Mech.* 272: 255–284 (1994).